J Nanopart Res (2017) 19: 347
DOI 10.1007/s11051-017-4021-5

RESEARCH PAPER

Morphological diversity of block copolymer/lipid chimeric nanostructures

Nikolaos Naziris · Natassa Pippa · Varvara Chrysostomou · Stergios Pispas · Costas Demetzos · Marcin Libera · Barbara Trzebicka

Received: 26 June 2017 / Accepted: 7 September 2017 / Published online: 18 October 2017

Abstract Different in nature biomaterials, which are used for the development of drug delivery nanosystems, could be mixed, in order to produce chimeric/mixed nanostructures. Their morphological characteristics and biophysical properties depend on the degree of association and interactions between the self-assembling biomaterials. For the purpose of this study, chimeric nanosystems composed of phospholipid and amphiphilic diblock copolymers were developed, at different molar ratios. Light scattering and imaging techniques were employed, in order to extract information on the nanostructure physicochemical characteristics and their morphology. Certain morphological characteristics were assessed for vesicle membranes, which are considered to be of paramount importance for their fate inside the physiological environment and their biophysical behavior. Besides vesicles, a variety of structures appeared in the phospholipid/copolymer chimeric systems, depending on both the composition and the concentration of the utilized polymer, declaring the lyotropic effect on the self-assembly of the biomaterials. The size range of most objects, including vesicles, was around 100 nm. Membrane irregularities, such as domains and rafts, are considered as functional biophysical factors, rendering liposomes appropriate artificial models for approaching various diseases on the level of living cell membranes. Such information is of paramount importance for the utilization of chimeric nanostructures in drug delivery and in therapy.

Keywords Block copolymer · Lipid · Cryo-TEM · Nanostructures

N. Naziris · N. Pippa · C. Demetzos (✉)
Section of Pharmaceutical Technology, Department of Pharmacy, School of Health Sciences, National and Kapodistrian University of Athens, Panepistimioupolis Zografou, 15771 Athens, Greece
e-mail: demetzos@pharm.uoa.gr

N. Pippa · V. Chrysostomou · S. Pispas (✉)
Theoretical and Physical Chemistry Institute, National Hellenic Research Foundation, 48 Vassileos Constantinou Avenue, 11635 Athens, Greece
e-mail: pispas@eie.gr

M. Libera · B. Trzebicka (✉)
Centre of Polymer and Carbon Materials, Polish Academy of Sciences, 34 ul. M. Curie-Skłodowskiej, 41-819 Zabrze, Poland
e-mail: btrzebicka@cmpw-pan.edu.pl

Introduction

Chimeric/mixed nanostructures, composed of different in nature biomaterials (e.g., lipids and polymers), are considered as innovative drug delivery nanosystems (Schulz and Binder 2015; Naziris et al. 2016). Recently developed imaging techniques offer a new approach on nanosystem examination and membrane morphology assessment and comprehension. Because of that, the result of lipid-polymer intermolecular interactions on the self-organization and final features of supramolecular structures may now be observed and even quantified (Zhong and Pochan 2010; Colombo et al. 2015).

As proposed by Bowick and Sknepnek, flat surfaces, like facets, might be easier than curved ones to functionalize, in order to facilitate biochemical reactions between drug delivery nanosystems and their targets (Bowick and Sknepnek 2013). More recently, the importance of synaptic vesicle membrane phase state on the binding of α-synuclein presynaptic protein was studied, indicating that a negatively charged membrane in the phase transition range or in the liquid-crystalline state promotes that binding and thus its own stability in the presynaptic gap. This may be related to neurodegenerative diseases, like Parkinson's, where aggregation of α-synuclein is suspected to play a role (Pirc and Ulrih 2015). Finally, protein insertion on polymer-lipid membranes was found to depend on the molar ratio of the two biomaterials, where control of topology and phase separation leads to selective protein distribution and provides specific spatial functionality (Kowal et al. 2015). These results highlight the importance of vesicle membrane polymorphism and morphology, which in turn relate to the biophysics of membranes. Information towards these lines allows for the rational development of drug delivery nanosystems and other bio-related applications.

To control structure morphology however, one must take into account the spontaneous self-assembly mechanisms, arising from the molecule nature in simple systems or from the compositional asymmetry of molecules in binary or higher mixtures. The co-assembly of different in elastic properties biomaterials leads to the generation of sphere-like vesicles, as well as other novel shapes, which result from the intermixture and later intramembrane asymmetric distribution of the amphiphiles producing high spontaneous curvature. In this manner, tubular vesicular morphologies for example may occur from the non-ideal mixing of amphiphiles, such as phospholipids and amphiphilic block copolymers, because of their different elastic properties, bending rigidity, etc., causing self-assembly to deviate from spherical vesicles. These tubes accommodate lipids in their core and polymers on their outer surface and apart from serving as biomimetic models for eukaryotic cell features, for the investigation of the role of lipids and other molecules in morphogenesis of cells and organelles; they can be also tailored for various biomedical and other applications (Lim et al. 2017). Apart from tubes, worm-like micelles have been reported in the literature, resulting from the mixing of lipids and polymers. Interestingly, in one of them, it was deduced that the polymer was accommodated in the core of the micelle, in opposition to the study of Lim et al. The architecture, molar mass, and molar ratio of the amphiphiles utilized are some of the critical parameters that define the type of morphology that will occur from the self-assembly process (Khan et al. 2016; Dao et al. 2017).

In the present investigation, our goal was to evaluate the concentration-dependent lyotropic effect on lipid/polymer self-assembled nanostructures and to identify their morphology. The accommodation of macromolecules inside the liposomal surface is known to influence the fluidity and polymorphism of the membrane, since these are lyotropic liquid crystalline systems. The biophysical mechanism of their formation will assist future studies to clarify their interactions with biological substrates, as well as to correlate their morphology and their surface "rafts" with human diseases (Binder et al. 2003).

We designed, developed, and studied chimeric nanosystems, comprised of phospholipid L-α-phosphatidylcholine, hydrogenated (Soy) (HSPC) (Fig. 1a) and two amphiphilic diblock copolymers, of the type poly(2-(dimethylamino)ethyl methacrylate)-b-poly(lauryl methacrylate) (PDMAEMA-b-PLMA 1 and 2) (Fig. 1b), which differ in their polymerization degree and molar composition. The first copolymer, with PDMAEMA/PLMA mass ratio 59:41, has a more hydrophilic balance, compared with the second, which has a 46:54 mass ratio. The HSPC lipid utilized has a phase transition temperature T_m = 51 ± 2 °C, while PDMAEMA exhibits thermo and pH-sensitive properties (Wei et al. 2016; Ward and Georgiou 2011; Samsonova et al. 2011). On the other hand, the PLMA segment possesses a long hydrophobic side chain that serves as a possible anchor of the copolymer inside the lipid bilayer. The chimeric vesicles were prepared in aqueous solution, in two lipid-polymer molar ratios for each polymer, 9:0.1 and 9:0.5 and studied with different techniques, in order to elucidate the polymer effect on their physicochemical characteristics, as well as the macroscopic morphology and microstructure of membrane. These data may provide a biophysical profile of the nanosystems, which can be correlated to co-assembly mechanisms and in the future, exploited for the prediction of their behavior in the physiological environment.

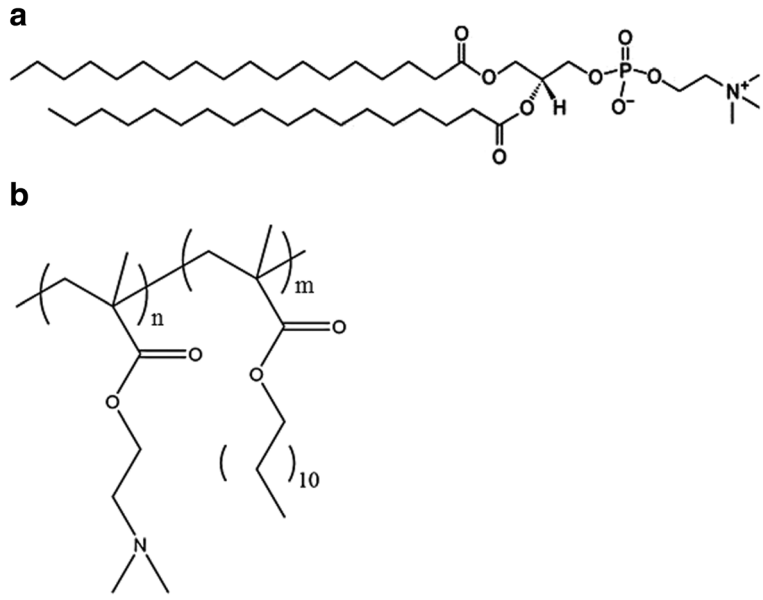

Fig. 1 Chemical structures of **a** HSPC phospholipid and **b** PDMAEMA-b-PLMA block copolymer. The segments' molar ratio (n/m) of the copolymers is 70:30 for the PDMAEMA-b-PLMA 1 and 58:42 for the PDMAEMA-b-PLMA 2 (PDMAEMA-b-PLMA 1: $n = 33$, $m = 15$, PDMAEMA-b-PLMA 2: $n = 32$, $m = 23$)

Materials and methods

Materials

The phospholipid L-a-phosphatidylcholine, hydrogenated (Soy) (HSPC) was purchased from Avanti Polar Lipids Inc. (Alabaster, AL, USA) and used without further purification. Chloroform and other reagents were of analytical grade and purchased from Sigma–Aldrich Chemical Co. The poly(2-(dimethylamino)ethyl methacrylate)-b-poly(lauryl methacrylate) (PDMAEMA-b-PLMA) amphiphilic diblock copolymers were synthesized by RAFT polymerization methodologies, in two different weight compositions, 59:41 for PDMAEMA-b-PLMA 1 and 46:54 for PDMAEMA-b-PLMA 2. The molar mass (M_w) of copolymers, determined by size exclusion chromatography, equates to 8900 and 10,800 g/mol, respectively. This gives a total of 33 DMAEMA and 15 LMA units for PDMAEMA-b-PLMA 1 and 32 DMAEMA and 23 LMA units for PDMAEMA-b-PLMA 2, i.e., the two diblocks have approximately the same PDMAEMA block length and PLMA blocks of different lengths.

Synthesis of poly(2-(dimethylamino)ethyl methacrylate)-b-poly(lauryl methacrylate) copolymers

The poly(2-(dimethylamino)ethyl methacrylate) (PDMAEMA) block was prepared first and then used as a macromolecular chain transfer agent for the synthesis of the second poly(lauryl methacrylate) (PLMA) block. A typical RAFT polymerization scheme for the synthesis of PDMAEMA homopolymer is described in the following: to a round-bottom flask (25 mL), (3 g, 19.1 mmol) 2-(dimethylamino)ethyl methacrylate (DMAEMA), (0.24 g, 0.6 mmol) 4-cyano-4-[(dodecylsulfanylthiocarbonyl)sulfanyl]pentanoic acid, (0.0098 g, 0.06 mmol) AIBN and 7 mL dioxane were added. The final solution was degassed by nitrogen gas bubbling for 15 min and subsequently left for polymerization at 65 °C for 18 h.

The RAFT polymerization procedure for the synthesis of the PDMAEMA-b-PLMA block copolymers is as follows: to a round-bottom flask (25 mL), (0.5/1.0 g, 1.96/3.93 mmol) lauryl methacrylate (LMA), (1.1/1.0 g, 0.224/0.198 mmol) poly(2-(dimethylamino)ethyl methacrylate) (PDMAEMA 1/PDMAEMA 2), (0.0184/0.0163 g, 0.1121/0.0995 mmol) AIBN and 4.8/6.0 mL benzene were added. The final solution was degassed by nitrogen gas bubbling for 15 min and left for polymerization at 65 °C for 24 h. The molecular weights (M_w) of the diblock copolymers were 8900 and 10,800 and the M_w/M_n values 1.16 and 1.19 for PDMAEMA-b-PLMA 1 and PDMAEMA-b-PLMA 2, respectively. Both values were obtained by size exclusion chromatography (SEC), using narrow distribution PS standards for calibration. Composition of the copolymers

was determined by ^{1}H NMR spectroscopy (Pispas and Hadjichristidis 2003; Khougaz et al. 1995).

Preparation of chimeric systems

Different chimeric formulations of HSPC/PDMAEMA-b-PLMA 1 and 2 have been prepared using the thin-film hydration method. Briefly, appropriate amounts of HSPC and PDMAEMA-b-PLMA 1/2 (9:0.1 and 9:0.5) were dissolved in chloroform/methanol (9:1 *v*/*v*) and then transferred into a round flask connected to a rotary evaporator (Rotavapor R-114, Buchi, Switzerland). Vacuum was applied and the chimeric phospholipid/block copolymer thin film was formed by slow removal of the solvent at 41 °C. The mixed film was maintained under vacuum for at least 24 h in a desiccator to remove traces of solvent. Subsequently, it was hydrated with PBS (*pH* = 7.4), by slowly stirring for 1 h in a water bath, above the phase transition temperature of the lipid (52 °C for HSPC), for a total concentration of 5 mg/mL. The resultant structures (apparently multilamellar vesicles, MLVs) were subjected to two 5-min sonication cycles (amplitude 70%, cycle 0.5 s) interrupted by a 5-min resting period, in a water bath, using a probe sonicator (UP 200S, dr. Hielsher GmbH, Berlin, Germany). The resultant chimeric nanostructures were allowed to anneal for 30 min.

Light scattering techniques

The diameter, size distribution, and ζ-potential of obtained nanostructures were investigated by dynamic and electrophoretic light scattering (DLS and ELS). For DLS and ELS, 100 μl of aliquots were 30-fold diluted in HPLC-grade water. Measurements are performed at a detection angle of 90° and at 25 °C, in a photon correlation spectrometer (Zetasizer 3000 HSA, Malvern, UK), and analyzed by CONTIN method (MALVERN software). Details on the methods have been published elsewhere (Pippa et al. 2013; Pippa et al. 2014).

Statistical analysis

Results from light scattering are shown as mean value ± standard deviation (SD) of three independent measurements. Statistical analysis was performed, using Student's *t* test, and multiple comparisons were done, using one-way ANOVA. *P* values < 0.05 were considered statistically significant. All statistical analyses were performed using Microsoft Excel.

Atomic force microscopy

For atomic force microscopy (AFM) measurements aqueous dispersions were spin coated onto mica surface using a standard spin coater model SPIN150, SPS-Europe B.V. (the Netherlands) with 400 rpm for 600 min and then samples were dried at room temperature for 24 h. AFM images were obtained using a MultiMode with Nanoscope IIId controller, Veeco (USA) AFM equipped with a piezoelectric scanner with a scan range of 10 × 10 μm^2. The imaging of samples was conducted in the tapping mode in ambient air conditions at a scan rate of 1 Hz using etched silicon probes (TESP, BRUKER) of nominal spring constant 42 N/m and operating at a resonant frequency of 320 kHz. All samples were imaged at room temperature. The Veeco NanoScope V531r1 program was employed to analyze the recorded images.

Cryogenic transmission electron microscopy

Cryogenic transmission electron microscopy (Cryo-TEM) micrographs were obtained using a Tecnai F20 TWIN microscope (FEI Company, USA) equipped with field emission gun, operating at an acceleration voltage of 200 kV. Images were recorded on the Eagle 4 k HS camera (FEI Company, USA) and processed with TIA software (FEI Company, USA). Specimen preparation was done by vitrification of the aqueous (HPLC-grade water) solutions on grids with holey carbon film (Quantifoil R 2/2; Quantifoil Micro Tools GmbH, Germany). Prior to use, the grids were activated for 30 s in oxygen plasma using a Femto plasma cleaner (Diener Electronic, Germany). Cryo-samples were prepared by applying a droplet (2.1 μL) of the solution to the grid, blotting with filter paper and immediate freezing in liquid ethane using a fully automated blotting device Vitrobot Mark IV (FEI Company, USA). After preparation, the vitrified specimens were kept under liquid nitrogen until they were inserted into a cryo-TEM-holder Gatan 626 (Gatan Inc., USA) and analyzed in the TEM at -178 °C. Pictures were processed using ImageJ software.

Results and discussion

Dynamic light scattering and electrophoretic light scattering of HSPC:PDMAEMA-b-PLMA chimeric systems

The details of physicochemical properties of chimeric vesicles are presented in Table 1. The D_h values show that the incorporation of either type of polymer led to chimeric vesicles of increased size. The *ζ-potential* values were found to be more positive for the chimeric vesicles (around 10–20 mV), compared to the conventional liposomes, which is attributed to the partially protonated amino groups of PDMAEMA at the hydration medium pH = 7.4. Concerning the last system, which exhibited disproportionate size and charge increase, we suspect that the high hydrophobicity of the particular copolymer, combined with the overcoming of a certain critical concentration threshold, led to the self-assembly and formation of larger polymer aggregates that hide the amino groups. This assessment is supported by the following presented results, especially cryo-TEM.

Atomic force microscopy of HSPC/PDMAEMA-b-PLMA chimeric systems

AFM was employed in order to assess the particle diameter, in the case of spherical structures, through calculating the horizontal distance of the cap-like structures formed by adsorption of the prepared vesicles on the surface coating (Winzen et al. 2013). The drying process may influence the vesicle shape, sometimes rather dramatically. The representative AFM micrographs of small and large objects of the HSPC/PDMAEMA-b-PLMA chimeric systems are given in Fig. 2, while the average diameters of the vesicles, extracted by calculation of the horizontal distances of the cap-like structures, are listed in Table 2. All chimeric system objects revealed on the micrographs were differentiated into two fractions. Small objects are of diameter 100–130 nm, whereas their height is 20–28 nm. The large objects, distinguished on the AFM micrographs, are of average diameter above 200 nm and height range 30–80 nm. In combination with cryo-TEM results, the fraction of small objects is assigned to liposomes, while that of large ones represents polymersomes.

Cryogenic transmission electron microscopy investigation of HSPC/PDMAEMA-b-PLMA morphologies

Different types of aggregated objects formed by HSPC/PDMAEMA-b-PLMA chimeric systems in PBS solution were visualized, using cryo-TEM methodology. Species present in solution can be preserved in their hydrated state, due to vitrification during cryo-preparation by plunge freezing. The vitrification process is carried out under controlled conditions, in order to avoid changes in solution concentration. The transparent film, formed by the amorphous ice, allows observation of the objects contained in the film.

The micrographs recorded for the chimeric systems are presented in Figs. 3 and 4. Images provide particular morphology information, like their size, size distribution, and thickness of walls. Some of the pictures also contain black dots of size around 15 nm. Such objects might originate from ice contamination, appearing

Table 1 Average diameter, polydispersity index, and ζ-potential of HSPC/PDMAEMA-b-PLMA chimeric systems, measured by DLS and ELS

Sample	Molar ratio	D_h[a] (nm)	SD[b]	ζ-pot[c] (mV)	SD
HSPC	–	104.0	0.4	2.2	0.6
HSPC/PDMAEMA-b-PLMA 1	9:0.1	134.0	1.0	11.0	6.9
HSPC/PDMAEMA-b-PLMA 1	9:0.5	145.2	0.4	19.0	5.2
HSPC/PDMAEMA-b-PLMA 2	9:0.1	124.6	1.0	20.7	0.4
HSPC/PDMAEMA-b-PLMA 2	9:0.5	188.2	2.9	10.6	4.8

[a] Hydrodynamic diameter

[b] Standard deviation

[c] ζ-potential

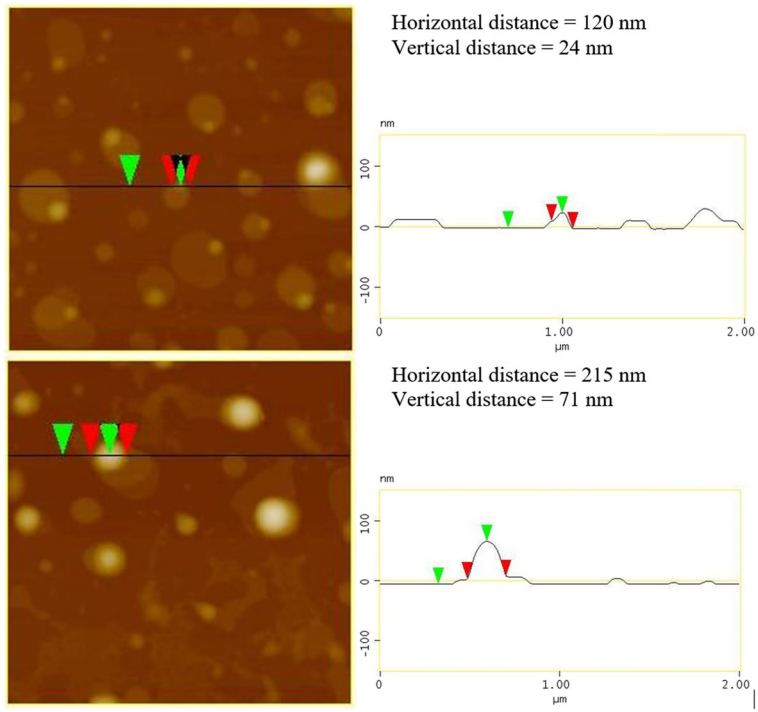

Fig. 2 AFM micrographs for fraction of small objects (top) and large objects (bottom), for the chimeric system of HSPC/PDMAEMA-b-PLMA 2 9:0.1

during cryo-preparation. However, taking into account that they appear only in the case of PDMAEMA-b-PLMA 1, they could also be polymer or chimeric/mixed sphere-like micelles, each resulting from the self-assembly of a small number of polymer chains. This hypothesis is strengthened by the fact that this copolymer has a large hydrophilic segment, which most likely acts as a driving force for the thermodynamic formation of hydrophobic core micelles during film hydration.

Pictures recorded for the studied chimeric systems reveal different kinds of aggregated species. All morphologies disclosed in cryo-TEM micrographs were differentiated according to their shape, size, and intensity profile of walls, based on a method presented elsewhere (Bermudez et al. 2002). The vesicles of different membrane composition and other morphologies (disc-like and worm-like structures) can be distinguished rather easily. The vesicles of angular shape, having uniform membrane thickness and uniform high electron beam contrast of the whole membrane, are ascribed as "homogeneous membrane" liposomes (Figs. 3 and 4, pointed by white arrow). Larger rounded vesicles, with thicker membrane, uniform thickness and uniform moderate contrast in whole membrane are ascribed as homogeneous membrane polymersomes (Figs. 3 and 4, pointed by blue arrow). The term "heterogeneous membrane" is used for either liposomes or polymersomes having "patchy" membrane, composed of segments having high and moderate electron contrast, which, in the case of polymersomes, vary in thickness

Table 2 Diameters of HSPC/PDMAEMA-b-PLMA chimeric systems measured by AFM

Sample	Molar ratio	Small fraction (nm)		Large fraction (nm)	
		Average diameter	Average height	diameter range	Height range
HSPC/PDMAEMA-b-PLMA 1	9:0.1	120	28	160–240	50–70
HSPC/PDMAEMA-b-PLMA 1	9:0.5	130	20	200–230	60–75
HSPC/PDMAEMA-b-PLMA 2	9:0.1	100	25	130–230	30–80
HSPC/PDMAEMA-b-PLMA 2	9:0.5	110	20	180–280	50–80

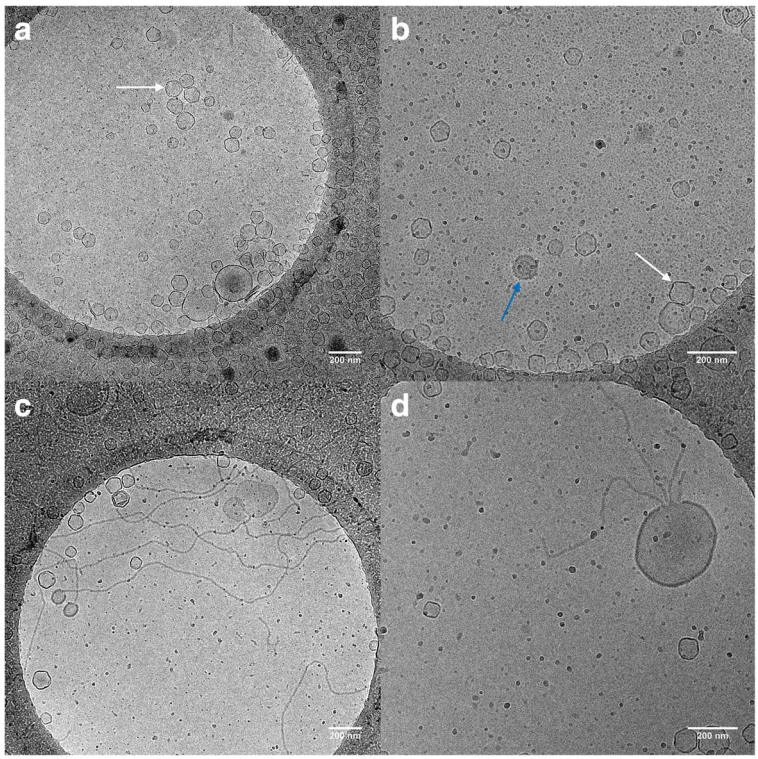

Fig. 3 Cryo-TEM images of aggregates of HSPC/PDMAEMA-b-PLMA 1 chimeric systems, in molar ratios 9:0.1 (**a**, **b**) and 9:0.5 (**c**, **d**)

(Fig. 5). The sizes of objects visible in cryo-TEM images were measured (Table 3). The number of similar objects was counted, to obtain the statistics for each category of structures (last column of Table 3).

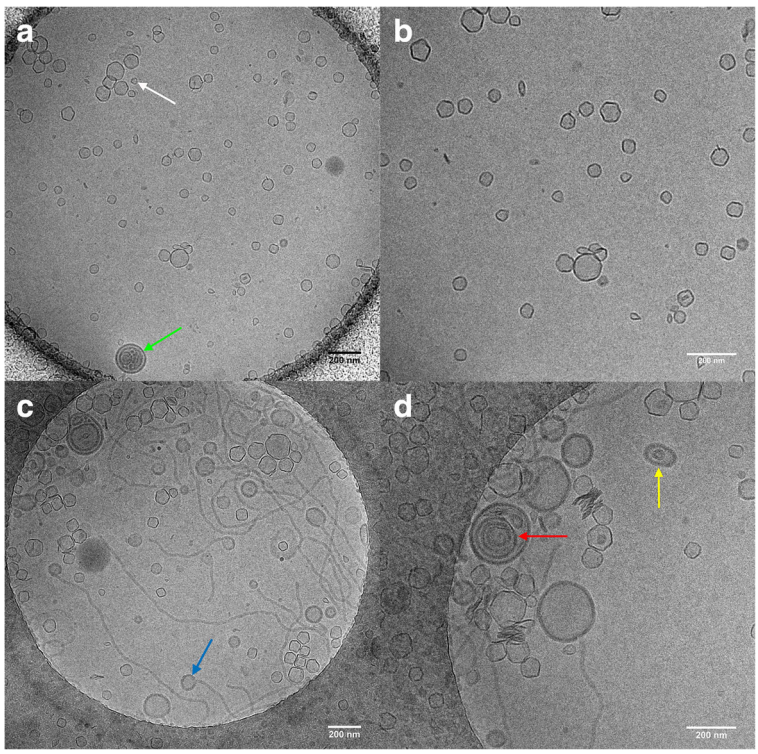

Fig. 4 Cryo-TEM images of aggregates of HSPC/PDMAEMA-b-PLMA 2 chimeric systems, in molar ratios 9:0.1 (**a**, **b**) and 9:0.5 (**c**, **d**)

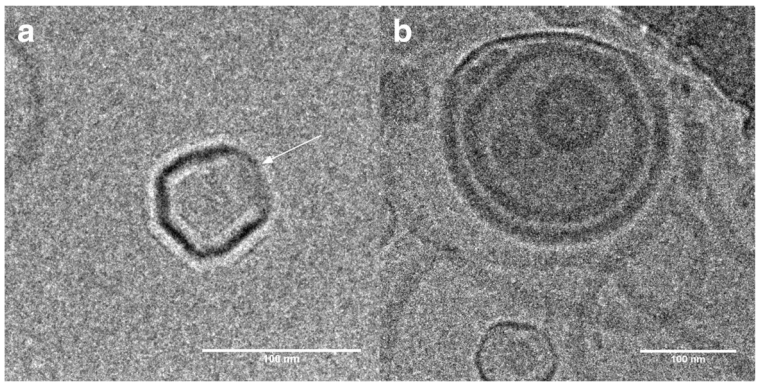

Fig. 5 Cryo-TEM images of heterogeneous membrane liposome (**a**) and heterogeneous membrane polymersome (**b**), occurring in the HSPC:PDMAEMA-b-PLMA 2 9:0.5 mixture

Liposomes of uniform membrane contrast ("homogeneous membrane") and angular shape (faceting) are the predominant kind of structures (Figs. 3 and 4, pointed by white arrow). The membrane thickness of such structures is around 6 nm for all dispersions. Such dimension is a bit larger than the 4–5 nm membrane thickness observed elsewhere for liposomes (Kuntsche et al. 2010; Kuntsche et al. 2011). Based on previous works, we believe that liposomes observed here are composed predominantly of HSPC lipids, probably incorporating a small amount of copolymer chains. Combination of materials, which construct the vesicles, as well as the distribution of the copolymer inside the lipid bilayer are presented elsewhere (Pippa et al. 2016; Koman et al. 2016). According to those results, it is possible that raft-like nanodomains, arising from inhomogeneous distribution of the polymer, are present on the vesicles or the copolymer is homogeneously distributed inside the liposomal membrane. The average diameter of these liposomes is similar in all samples (69–80 nm). The faceting of the lipid bilayer can be related to the conditions of cryo-TEM preparation, where samples, before plunge freezing, are incubated below the liposomal membrane transition temperature T_m (51 ± 2 °C for HSPC) and exist in their gel phase. However, a previous study that utilized HSPC did not record this phenomenon until the size of vesicles was too small, namely, 40 nm, and another suggested that cholesterol-free liposomes do not easily adopt a faceted conformation above 100 nm (Kaiser et al. 2003; Ickenstein et al. 2006). In this case, maybe the currently observed faceting is promoted by the insertion of polymer inside the membrane and is related with nanodomains (Bowick and Sknepnek 2013; Tribet and Vial 2008).

Second family of structures are vesicles (polymersomes) of uniform membrane contrast and thickness ("homogeneous membrane"); however, their size is larger, membrane contrast is lower, and membrane thickness (13–15 nm) is higher than liposomes (Figs. 3 and 4, pointed by blue arrow). The presence of PDMAEMA-b-PLMA 2 led to membranes of slightly higher thickness, correlated with the higher molar mass of the second copolymer, compared with the first (Itel et al. 2014). Similar structures were previously described in polymer-lipid systems and were related to chimeric/mixed polymer-lipid vesicles (Schulz and Binder 2015; Winzen et al. 2013). Average diameter of considered vesicles is 116–154 nm. Slight difference in diameter of chimeric/mixed membrane formed in HSPC/PDMAEMA-b-PLMA 1 (116 and 131 nm, Table 3) and HSPC/PDMAEMA-b-PLMA 2 (close to 150 nm, Table 3) systems can be pointed out. Besides unilamellar, also multilamellar (Fig. 4d, pointed by red and yellow arrow) and multivesicular (Fig. 4a, pointed by green arrow) structures, composed of homogeneous membrane polymersomes can be recognized, similar with those of other polymer-lipid dispersions (Tribet and Vial 2008). The micrographs did not reveal faceting effect in the case of polymersomes, indicating that the high amount of membrane polymer could prevent the rigidity of gel state of lipids (Dao et al. 2015).

Besides vesicles of uniform membrane contrast, structures having patchy membrane (heterogeneous membrane), looking like composed of two kinds of membranes, can be recognized for both liposomes and polymersomes, the latter also exhibiting quite different intramembrane thickness (Fig. 5). The mechanism of membrane formation is not obvious. It has been shown in the literature that this phenomenon results from the different orientation of facets, regarding the electron beam angle, suggesting that these vesicles might be neat liposomes (Fig. 5a)

Table 3 Diameter and wall dimension of objects formed by HSPC/PDMAEMA-b-PLMA, measured with cryo-TEM

Sample	Molar ratio	Type of objects observed		Wall thickness or core diameter for worms[a] (nm)	Diameter or length for worms[a] (nm)	Quantity (%)
HSPC/PDMAEMA-b-PLMA 1	9:0.1	Liposomes	Homogeneous membrane[d]	6.1	69.3	94.8
			Heterogeneous membrane[e]			0.2
		Polymersomes	Homogeneous membrane[f]	12.8[b]	116.1[b]	3.9
			Heterogeneous membrane[g]	13.1/6.0[c]		0.1
		Disk-like structures		26.3[b]	117.3[b]	1
		Worm-like micelles		–	–	0
HSPC/PDMAEMA-b-PLMA 1	9:0.5	Liposomes	Homogeneous membrane	5.8	80.1	85.8
			Heterogeneous membrane			0.2
		Polymersomes	Homogeneous membrane	13.1	131.7	6.9
			Heterogeneous membrane	13.6/6.1[c]		0.1
		Disk-like structures		31.5	115.4	2
		Worm-like micelles		13.2	> 1000	5
HSPC/PDMAEMA-b-PLMA 2	9:0.1	Liposomes	Homogeneous membrane	5.7	69.9	91.8
			Heterogeneous membrane			0.2
		Polymersomes	Homogeneous membrane	13.7[b]	154.3[b]	3.8
			Heterogeneous membrane	14.2/6.0[c]		0.2
		Disk-like structures		35.0	147.6	2
		Worm-like micelles		14.9[b]	~ 800[b]	2
HSPC/PDMAEMA-b-PLMA 2	9:0.5	Liposomes	Homogeneous membrane	5.8	75.5	50.5
			Heterogeneous membrane			0.5
		Polymersomes	Homogeneous membrane	15.1	149.4	24.6
			Heterogeneous membrane	16.0/5.9[c)]		0.4
		Disk-like structures		38.3	128.2	3
		Worm-like micelles		15.3	> 1000	21

[a] Calculated as average value of 100 aggregated structures

[b] Calculated as average value of 10 aggregated structures, due to small amounts of objects

[c] Average thickness of membrane segments with moderate contrast/average thickness of membrane segments with high contrast

[d] Liposomes with a membrane with homogeneous contrast

[e] Liposomes with a membrane with heterogeneous contrast

[f] Polymersomes with a membrane with homogeneous contrast

[g] Polymersomes with a membrane with heterogeneous contrast

(Andersson et al. 1995). However, this cannot be the case for certain objects, characterized by membrane thickness difference of segments on the same vesicle (Fig. 5b). Another approach attributes the variation in thickness of liposomal membrane to nanoscale phase segregation and the formation of observable copolymer or lipid domains, for liposomes and polymersomes, respectively (Dao et al. 2017).

Disc-shaped objects can be found only seldom on the micrographs (Figs. 3a and 4d). Their thickness is slightly higher than two times the membrane of polymersomes. This may indicate that discs are formed by compressing polymersomes. Kuntsche et al. observed disc-like structures, particularly micelles, varying in size and shapes, from small rods having high contrast to circular structures of lower contrast (Kuntsche et al. 2011). It has been demonstrated that the disc formation can be enhanced by phospholipid hydrolysis or heating gel phase vesicles above their phase transition, as well as by composition of mixture, way of preparation, thermal pre-treatment, or storage condition (Ickenstein et al. 2006).

In cryo-TEM micrographs, one can distinguish worm-like objects (Figs. 3c, d and 4c, d), predominantly in cases of lipid/copolymer systems with molar ratio 9:0.5. No worms were found for sample HSPC/PDMAEMA-b-PLMA 1 9:0.1, whereas in the case of HSPC/PDMAEMA-b-PLMA 2 9:0.1, only several worm-like objects could be disclosed. The worm thickness/core diameter of several nanometers corresponds well with the membrane thickness of polymersomes. Worm-like micelles have been previously reported for lipid/PEGylated lipid systems (Johnsson and Edwards 2003 Sandström et al. 2007; Vaccaro et al. 2007), as well as for chimeric systems of lipids and amphiphilic block copolymers (Khan et al. 2016; Dao et al. 2017).

Cryo-TEM micrographs indicate that polymersomes, as well as discs and worms, occur predominantly in cases of higher molar ratio of copolymer to phospholipid (9:0.5), further confirming the contribution of copolymers in the formation of these structures. Moreover, the nature of the copolymer is a determining factor for the formation of such self-assembled morphologies as well, as deduced from their content in the case of HSPC/PDMAEMA-b-PLMA 2 systems, PDMAEMA-b-PLMA 2 being more hydrophobic. These observations denote the dual concentration and composition-dependent formation of non-vesicular aggregates in chimeric lyotropic systems developed by two different types of amphiphilic biomaterials, such as lipid and block copolymer molecules.

Conclusion

Lyotropism of biomaterials, dependent on their concentration for producing chimeric liquid crystals, has emerged as an innovative approach in drug delivery and in therapeutics. Different in morphology chimeric objects have been observed and studied by using light scattering, AFM, and cryo-TEM techniques. The nature of the copolymers used, i.e., hydrophilic-to-hydrophobic balance and their lyotropism are responsible for the generation of structural and morphological diversity. This observation denotes the necessity to control the development protocols that influence the self-assembly process of chimeric/mixed nanosystems. However, their formation gives us the opportunity to study and comprehend the great morphological diversity that emerges from slight differences in nanoscale properties and in surface thermodynamics.

In the present study, cryo-TEM figures showed that chimeric/mixed soft matter nanostructures could present bio-morphological characteristics, which can be taken into account during the design and evaluation process of lyotropic drug delivery nanosystems. Domain and raft formation in vesicles should be assessed, as it plays an important role in their interactions with physiological membranes and their membrane conformation, with respect to angular morphologies, might affect their biophysical behavior. In addition, membrane irregularities that occur due to the incorporation of amphiphilic molecules in the liposomal bilayer, like block copolymers, may contribute to our understanding of the physiological membrane morphology complexity and its role in biological interactions. Overall, chimeric liposomes, due to their dynamic liquid crystal surface and unique morphology, can serve as artificial bio-models for approaching human diseases, where domains have been identified as biophysical disease factors, while on the other hand, they can be controlled to produce ideal drug delivery systems.

Compliance with ethical standards

Conflict of interest The authors declare that they have no conflict of interest.

References

Andersson M, Hammarstroem L, Edwards K (1995) Effect of bilayer phase transitions on vesicle structure, and its influence on the kinetics of viologen reduction. The J Phys Chem 99:14531–14538

Bermudez H, Brannan AK, Hammer DA, Bates FS, Discher DE (2002) Molecular weight dependence of polymersome membrane structure, elasticity, and stability. Macromolecules 35: 8203–8208

Binder WH, Barragan V, Menger FM (2003) Domains and rafts in lipid membranes. Angew Chem Int Ed 42:5802–5827

Bowick MJ, Sknepnek R (2013) Pathways to faceting of vesicles. Soft Matter 9:8088–8095

Colombo S, Cun D, Remaut K, Bunker M, Zhang J, Martin-Bertelsen B, Yaghmur A, Braeckmans K, Nielsen HM, Foged C (2015) Mechanistic profiling of the siRNA delivery dynamics of lipid–polymer hybrid nanoparticles. J Control Release 201:22–31

Dao TPT, Fernandes F, Er-Rafik M, Salva R, Schmutz M, Brûlet A, Prieto M, Sandre O, Le Meins JF (2015) Phase separation

and nanodomain formation in hybrid polymer/lipid vesicles. ACS Macro Lett 4:182–186

Dao TPT, Brûlet A, Fernandes F, Er-Rafik M, Ferji K, Schweins R, Chapel JP, Fedorov A, Schmutz M, Prieto M, Sandre O, Le Meins JF (2017) Mixing block copolymers with phospholipids at the nanoscale: from hybrid polymer/lipid wormlike micelles to vesicles presenting lipid nanodomains. Langmuir 33:1705–1715

Ickenstein LM, Sandström MC, Mayer LD, Edwards K (2006) Effects of phospholipid hydrolysis on the aggregate structure in DPPC/DSPE-PEG2000 liposome preparations after gel to liquid crystalline phase transition. Biochim Biophys Acta 1758:171–180

Itel F, Chami M, Najer A, Lörcher S, Wu D, Dinu IA, Meier W (2014) Molecular organization and dynamics in polymersome membranes: a lateral diffusion study. Macromolecules 47:7588–7596

Johnsson M, Edwards K (2003) Liposomes, disks, and spherical micelles: aggregate structure in mixtures of gel phase phosphatidylcholines and poly(ethylene glycol)-phospholipids. Biophys J 85:3839–3847

Kaiser N, Kimpfler A, Massing U, Burger AM, Fiebig HH, Brandl M, Schubert R (2003) 5-Fluorouracil in vesicular phospholipid gels for anticancer treatment: entrapment and release properties. Int J Pharm 256:123–131

Khan S, Li M, Muench SP, Jeuken LJ, Beales PA (2016) Durable proteo-hybrid vesicles for the extended functional lifetime of membrane proteins in bionanotechnology. Chem Commun (Camb) 52:11020–11023

Khougaz K, Astafieva I, Eisenberg A (1995) Micellization in block polyelectrolyte solutions. 3. Static light scattering characterization. Macromolecules 28:7135–7147

Kolman I, Pippa N, Meristoudi A, Pispas S, Demetzos C (2016) A dual-stimuli-responsive polymer into phospholipid membranes. J Therm Anal Calorim 123:2257–2271

Kowal J, Wu D, Mikhalevich V, Palivan CG, Meier W (2015) Hybrid polymer−lipid films as platforms for directed membrane protein insertion. Langmuir 31:4868–4877

Kuntsche J, Freisleben I, Steiniger F, Fahr A (2010) Temoporfin-loaded liposomes: physicochemical characterization. Eur J Pharm Sci 40:305–315

Kuntsche J, Horst JC, Bunjes H (2011) Cryogenic transmission electron microscopy (cryo-TEM) for studying the morphology of colloidal drug delivery systems. Int J Pharm 417:120–137

Lim SK, Wong ASW, de Hoog HPM, Rangamani P, Parikh AN, Nallani M, Sandin S, Liedberg B (2017) Spontaneous formation of nanometer scale tubular vesicles in aqueous mixtures of lipid and block copolymer amphiphiles. Soft Matter 13:1107–1115

Naziris N, Pippa N, Pispas S, Demetzos C (2016) Stimuli-responsive drug delivery Nanosystems: from bench to clinic. Curr Nanomed 6:166–185

Pippa N, Kaditi E, Pispas S, Demetzos C (2013) PEO-b-PCL-DPPC chimeric nanocarriers: self-assembly aspects in aqueous and biological media and drug incorporation. Soft Matter 9:4073–4082

Pippa N, Deli E, Mentzali E, Pispas S, Demetzos C (2014) PEO-b-PCL grafted DPPC liposomes: physicochemical characterization and stability studies of novel bio-inspired advanced drug delivery nano systems (aDDnSs). J Nanosci Nanotechnol 14:5676

Pippa N, Stellas D, Skandalis A, Pispas S, Demetzos C, Libera M, Marcinkowski A, Trzebicka B (2016) Chimeric lipid/block copolymer nanovesicles: Physico-chemical and biocompatibility evaluation. Eur J Pharm Biopharm 107:295–309

Pirc K, Ulrih NP (2015) α-Synuclein interactions with phospholipid model membranes: key roles for electrostatic interactions and lipid-bilayer structure. Biochim Biophys Acta 1848:2002–2012

Pispas S, Hadjichristidis N (2003) Micellization behavior of poly(-butadiene-*b*-sodium methacrylate) copolymers in dilute aqueous media. Macromolecules 36:8732–8737

Samsonova O, Pfeiffer C, Hellmund M, Merkel OM, Kissel T (2011) Low molecular weight pDMAEMA-*block*-pHEMA block-copolymers synthesized via RAFT-polymerization: potential non-viral gene delivery agents? Polymers 3:693–718

Sandström MC, Johansson E, Edwards K (2007) Structure of mixed micelles formed in PEG-lipid/lipid dispersions. Langmuir 23:4192–4198

Schulz M, Binder WH (2015) Mixed hybrid lipid/polymer vesicles as a novel membrane platform. Macromol Rapid Commun 36:2031–2014

Tribet C, Vial F (2008) Flexible macromolecules attached to lipid bilayers: impact on fluidity, curvature, permeability and stability of the membranes. Soft Matter 4:68–81

Vaccaro M, von Corswant C, Söderman O (2007) Investigation of the adsorption of PEG1500-12-acyloxystearate surfactants onto phospholipid bilayers: an ellipsometry and Cryo-TEM study. Biophys J 93:4300–4306

Ward MA, Georgiou TK (2011) Thermoresponsive polymers for biomedical applications. Polymers 3:1215–1242

Wei X, Cohen R, Barenholz Y (2016) Insights into composition/structure/function relationships of Doxil® gained from "high-sensitivity" differential scanning calorimetry. Eur J Pharm Biopharm 104:260–270

Winzen S, Bernhardt M, Schaeffel D, Koch A, Kappl M, Koynov K, Landfester K, Kroeger A (2013) Submicron hybrid vesicles consisting of polymer-lipid and polymer-cholesterol blends. Soft Matter 9:5883–5890

Zhong S, Pochan DJ (2010) Cryogenic transmission electron microscopy for direct observation of polymer and small-molecule materials and structures in solution. Polym Rev 50:287–320